Modeling the effect of clay drapes on pumping test response in a cross-bedded aquifer using multiple-point geostatistics

Marijke Huysmans[1] and Alain Dassargues[1,2]

Abstract This study investigates whether small-scale clay drapes can cause an anisotropic groundwater pumping test response at a much larger scale. The measured drawdown values from a pumping test in the cross-bedded Brussels Sands aquifer (Belgium) reveal an elliptical-shaped pumping cone. The major axis of the pumping ellipse is parallel with the strike of small-scale clay drapes that are observed and measured in several outcrops. This study investigates (1) whether this large-scale anisotropy can be the result of small-scale clay drapes and (2) whether application of multiple-point geostatistics can improve the analysis of pumping tests. This study uses the technique of "direct multiple-point geostatistical simulation of edge properties" which enables simulating thin irregularly-shaped surfaces with a smaller CPU and RAM demand than the conventional multiple-point statistical methods. The proposed method uses model cell edge properties for indicating the presence of thin irregularly-shaped surfaces. Instead of pixel values, model cell edge properties such as edge transmissibility indicating the presence of irregularly-shaped surfaces are simulated using the multiple-point geostatistical algorithm SNESIM. The modelling strategy of this study consists of the following steps. First, a training image displaying clay drape occurence is constructed. Secondly, this small grid cell size training image is converted into an upscaled edge training image which is used as input training image to perform SNESIM simulations. The resulting simulations indicate at which cell edges horizontal or vertical clay drapes are present. This information is incorporated in a local 3D groundwater model of the pumping test site by locally adapting vertical leakance values and by locally inserting horizontal flow barriers. All hydraulic parameters including the clay drapes properties are calibrated using the measured drawdown time series in six observation wells. Results show that the anisotropic pumping cone can be attributed to the presence of the clay drapes.

[1] KU Leuven, Department of Earth and Environmental Sciences, Celestijnenlaan 200E, 3001 Heverlee, Belgium, marijke.huysmans@ees.kuleuven.be

[2] Department of Architecture, Geology, Environment, and Civil Engineering (ArGEnCo), Université de Liège, Belgium, alain.dassargues@ulg.ac.be

1 Introduction

Clay drapes are thin irregularly-shaped layers of low-permeability material that are often observed in different types of sedimentary deposits. Their thicknesses are often only a few centimeters [12, 34]. Despite their limited thicknesses, several studies indicate that they may influence subsurface fluid flow and solute transport at different scales (16, 24, 25, 34, 36]. However, many studies show that the effect of small-scale heterogeneity is limited to small scales and averaged out on larger scales and that consequently the type of geological heterogeneity that needs to be taken into account depends on the scale of the problem under consideration [1, 7, 26, 30, 31]. This study therefore investigates whether small-scale clay drapes can cause an anisotropic pumping test response at a much larger scale. This study is based on measured drawdown values from a pumping that reveal an anisotropic or elliptical-shaped pumping cone. The major axis of the pumping ellipse is parallel with the strike of the centimeter to meter-scale clay drapes that are observed and measured in several outcrops and quarries. This study investigates whether this large-scale anisotropy can be the result of small-scale clay drapes.

The small size and the complexity of the shape and distribution of clay drapes makes it very difficult to incorporate them in aquifer or reservoir flow models. In standard upscaling approaches [8, 28], the continuity of the clay drapes is not preserved [34]. Multiple-point geostatistics is a technique that has proven to be very suitable for simulating the spatial distribution of such complex structures [2, 4, 5, 14, 16, 32, 33]. In large-scale three-dimensional grids this method may however be computationally very intensive. [17] therefore developed the method of "direct multiple-point geostatistical simulation of edge properties" which enables simulating thin irregularly-shaped surfaces with a smaller CPU and RAM demand than the conventional multiple-point statistical methods. This method has been applied on simple test cases [17] and the present study is the first to apply this method on a full-scale three-dimensional groundwater model. In this way, this study investigates whether the combined approach of using multiple-point geostatistics and edge properties is an efficient and valid method for integrating small-scale features in larger scale models.

A last goal of this paper is to determine the added benefits of explicitly incorporating clay drape presence for inverse modeling of pumping tests. Several authors have shown that incorporating heterogeneity can results in improved correspondence between calculated and observed hydraulic heads (e.g.,[10, 19, 20, 29]. However, some authors show that incorporating additional data about heterogeneity does not always results in better calibration results heads (e.g. [11]). This paper quantifies the change in calibration error when clay drapes are incorporated in groundwater flow models.

2 Material and methods

The methodology followed in this study consists of the following steps. First, field data is obtained in an extensive field campaign mapping sedimentary heterogeneity and small-scale air permeability. Secondly, a training image displaying clay drape occurrence is constructed based on the geological and hydrogeological field data obtained from this field campaign. Thirdly, this small grid cell size training image is converted into an upscaled edge training image which is used as input training image to perform SNESIM simulations. The resulting simulations indicate at which cell edges horizontal or vertical clay drapes are present. This information is incorporated in a local 3D groundwater model of the pumping test site by locally adapting vertical leakance values and by locally inserting horizontal flow barriers. All hydraulic parameters including the clay drapes properties are calibrated using the measured drawdown time series in six observation wells.

2.1 Geological setting

The pumping test site is situated in Bierbeek near Leuven (Belgium) as shown on Figure 1. The subsurface geology in this area consists of a 4m-thick cover of sandy loam from Pleistocene age, 35m of Middle-Eocene Brussels Sands and 12 m of low permeable Early-Eocene Ieper Clay. All pumping and observation wells of the pumping test are screened in the Brussels Sands. The Brussels Sands formation is an early Middle-Eocene shallow marine sand deposit in Central Belgium (Figure 1). Its geological features are extensively covered in [12] and [13]. This aquifer is a major source of groundwater in Belgium and was studied at the regional scale by [27]. The most interesting feature of these sands in terms of groundwater flow and transport is the complex geological heterogeneity originating in its depositional history. The Brussels Sands are a tidal sandbar deposit. Its deposition started when a strong SSW-NNE tidal current in the early Middle-Eocene produced longitudinal troughs, that were afterwards filled by sandbar deposits. In these sandbar deposits, sedimentary features such as cross-bedding, mud drapes and reactivation surfaces are abundantly present [12, 13]. The orientation of most of these structures is related to the NNE-orientation of the main tidal flow during deposition.
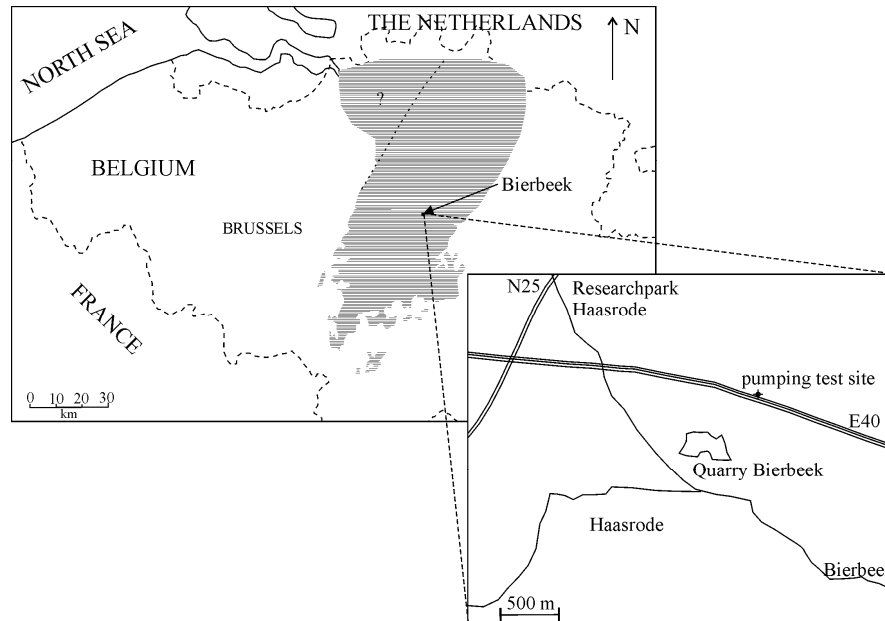
Figure 1 Map of Belgium showing Brussels Sands outcrop and subcrop area (shaded part) (modified after [12] and inset showing the location of the pumping test site and the Bierbeek quarry

2.2 Pumping test

In February 1993, a pumping test was performed in Bierbeek (Belgium) under the authority of the company TUC RAIL N.V. in the framework of high-speed train infrastructure works. One pumping well (PP1) and six observations wells were constructed in the 35m-thick coarse facies of the Brussels Sands (Figure 2). The pumping test was interpreted by inverse modeling using a numerical method described in [21]. This analysis showed that the best calibration was obtained assuming horizontal anisotropy in the coarse facies of the Brussels Sands. The principal direction of maximal horizontal hydraulic conductivity corresponds to N 115°48' E [35]. This principal orientation is exactly perpendicular to the SSW-NNE orientation of the main tidal flow during deposition and the mud drapes in the Brussels Sands.
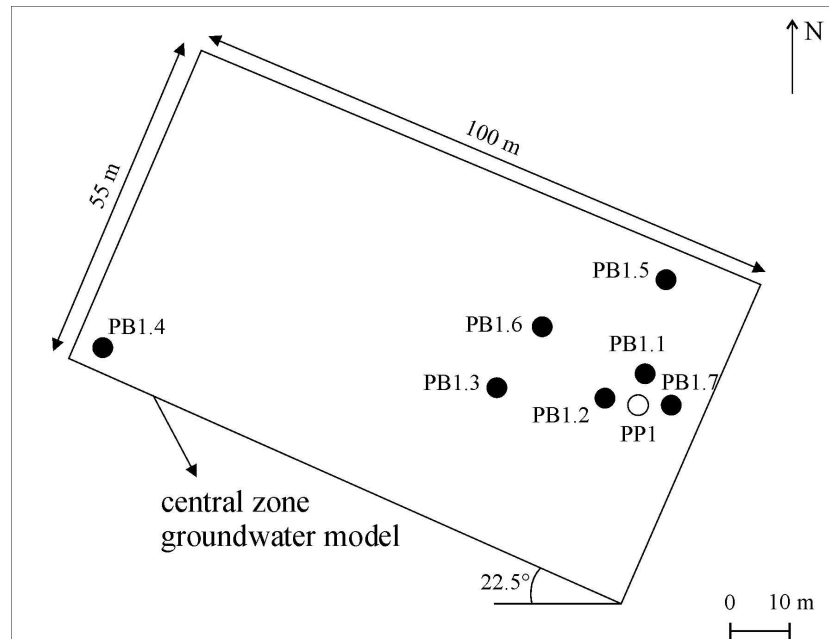
Figure 2 Pumping test configuration showing the pumping well (white circle) and observation wells (black circles) and the orientation and delineation of the central inner zone of the local groundwater model

2.3 In situ mapping and measurement of clay drape properties

The Brussels Sands outcrops in the Bierbeek quarry are used as an analog for the Brussels Sands found in the subsurface at the pumping test site. This quarry is located at approximately 500 m from the pumping test site (Figure 1). This outcrop of approximately 1200 m² was mapped in detail with regard to the spatial distribution of sedimentary structures and permeability in [18]. From the hydrogeological point of view in the present study, the main interest lies in the occurrence and geometry of structures with high and low hydraulic conductivity. In this perspective, the Brussels Sands can be regarded as consisting of horizontal permeable sand layers of approximately 1m thick intercalated by horizontal low-permeable clay-rich bottomsets and inclined low-permeable clay drapes. Figure 3 shows a field picture and a geological interpretation of the typical clay-sand patterns in the Bierbeek quarry. More details about the spatial distribution of the small-scale sedimentary structures and permeability in the Brussels Sands can be found in [18].
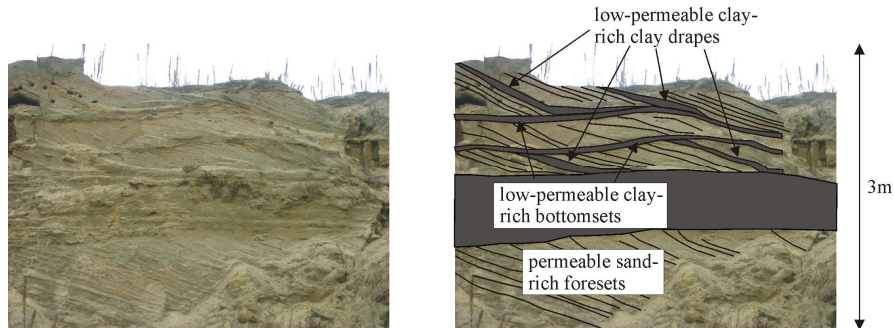
Figure 3 Field picture and interpreted field picture depicting foresets, bottomsets and clay drapes in the Brussels Sands observed in the Bierbeek quarry

2.4 Training image construction

Training images are essential to multiple-point geostatistics, which is a technique that has proven to be very suitable for simulation of such complex structures [2, 4, 14, 16, 32, 33]. In multiple-point geostatistics, "training images" are used to characterize the patterns of geological heterogeneity. In this study, a two-dimensional fine-scale training image of clay and sand occurrence of the Brussels Sands was constructed based on the in situ mapping in the Bierbeek quarry. The fine-scale training image along the NNE-direction (Figure 4) shows an alternation of sand-rich and clay-rich zones. More details about construction of this training image can be found in [16]. This training image will be used in section 2.6 where multiple-point statistics are borrowed from this training image to simulate realizations of clay drape occurrence to use as input for the local groundwater model.

2.5 Groundwater model

The groundwater model is a three-dimensional local model of 600m x 600 m x 30.4m including all pumping and observation wells from the pumping test in Bierbeek described in section 2.2. The model is oriented along the N22.5°E direction which is parallel to the direction of the main geological structures and the main anisotropy axis of the observed drawdowns from the pumping test. The model consists of a central inner zone of 55m x 100m x 15.3m including all well screens and an outer zone (Figure 7). This inner zone consists of 51 cells in the x-direction, 183 cells in the y-direction and 51 layers. In the central inner zone where all the well screens are situated, a very small grid cell size of 0.3m x 0.3m x

0.3m is adopted so that individual clay drapes can be explicitly incorporated in the model in this zone. In the outer zone, larger grid cell sizes between 0.45m and 82m in the horizontal direction and layer thicknesses between 3m and 6m are chosen. For numerical reasons, the dimensions of the grid cells do not exceed 1.5 times the dimensions of their neighboring cells. The total model consists of 213 cells in the x-direction, 361 cells in the y-direction and 54 layers. The total number of grid cells in the model is thus 4,152,222 cells. The model is run in transient conditions with a total time length of 4510 minutes subdivided into 99 time periods. Piezometric heads are prescribed at the boundaries of all model layers. In the pumping well PP1, a pumping rate of 2120 m³/day is applied during 72 hours. Initial hydraulic conductivity and storage parameters were taken from a previous interpretation [35] and calibrated afterwards. A total of 594 observed heads measured in six observation wells (Figure 2) from two minutes after the start of pumping until 240 minutes after stopping of pumping are available for calibration. The differential equations describing groundwater flow are solved by PMWIN [3], which is a pre- and post-processor for MODFLOW [23], using a block-centered, finite-difference method.

Two model variants are run and calibrated separately. First, a homogeneous and horizontally isotropic model without clay drapes is run. In this model, different values for horizontal and vertical hydraulic conductivity are allowed, but no anisotropy of hydraulic conductivity in the horizontal direction is introduced. Calibration is performed for adapting values of horizontal hydraulic conductivity, vertical hydraulic conductivity and specific storage.
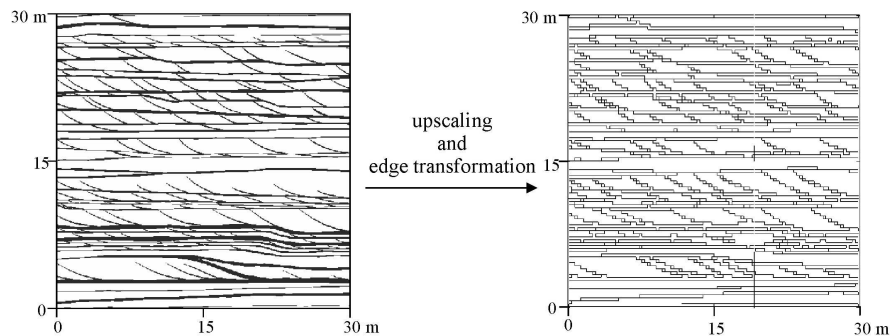

Figure 4 (left) Vertical two-dimensional training image of 30 m by 30 m in NNE direction: sand facies (white), clay-rich facies (black) modified from [16] and (right) the corresponding edge training image modified from [17]

The second model is a model incorporating a random clay drape realization as described in section 2.6. In this model, calibration of the following additional parameters is performed: clay drape thickness and clay drape hydraulic

conductivity in model layers 4 to 54 and anisotropy factor of layers 1 to 3 in which clay drapes are not explicitly incorporated. The spatial distribution of the clay drapes is not changed during calibration. In this model, the only heterogeneity and anisotropy of hydraulic conductivity is related to the presence of clay drapes. Background hydraulic conductivity of layers 4 to 54 is homogeneous and isotropic so that the effect of clay drapes on hydraulic heads can be determined without influence of other heterogeneity or anisotropy effects. By comparing the results of these two model variants, the effects of clay drapes on the piezometric depression cone and on the calibration results can be quantified. This approach of comparing a heterogeneous model with a homogeneous equivalent was also applied in [22]. For both models, a two-step calibration procedure is adopted. First, a sensitivity analysis and manual calibration is performed and second, the model is further calibrated using PEST [6].
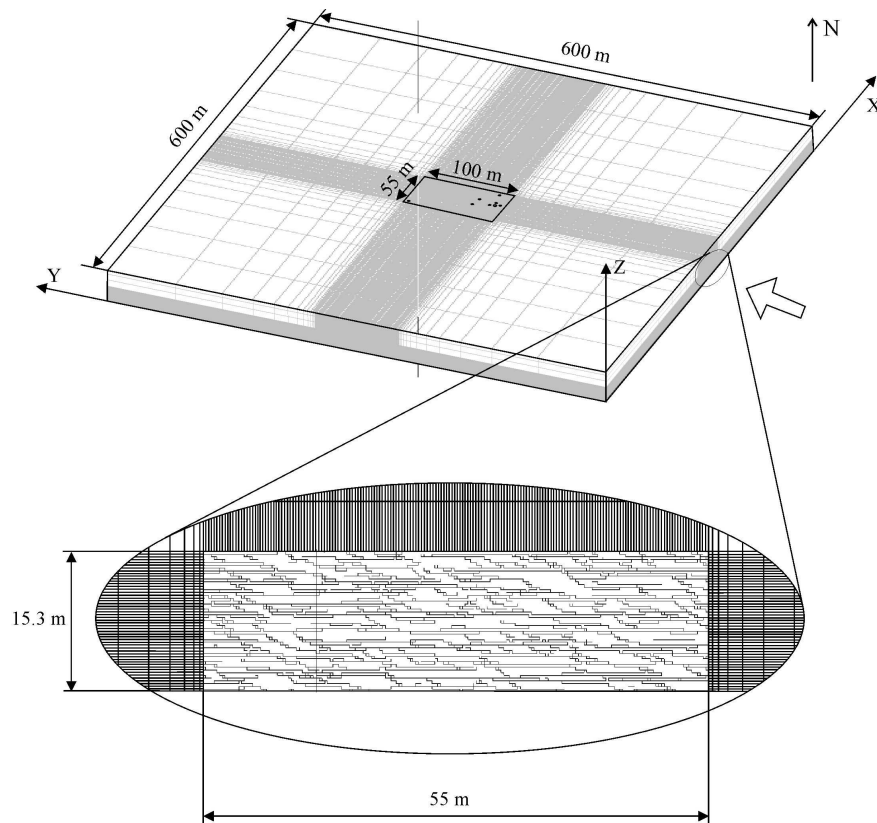

Figure 5 Groundwater flow model grid and edge realization

2.6 Clay drapes simulation using multiple-point geostatistical simulation of edge properties

In order to incorporate clay drapes showing patterns similar to the training image of Figure 4 (left) in the groundwater flow model, the technique of direct multiple-point geostatistical simulation of edge properties [17] is used. This technique was designed to simulate thin complex surfaces such as clay drapes with a smaller CPU and RAM demand than the conventional multiple-point statistical methods. Instead of pixel values, edge properties indicating the presence of irregularly-shaped surfaces are simulated using multiple-point geostatistical simulation algorithms. The training image is upscaled by representing clay drapes as edge properties between cells instead of representing them as objects consisting of several cells. The concept of the edge of a flow model and the associated edge properties was introduced in the work of [34] as an additional variable. The edge properties are properties assigned to the cell faces. The cell property defined in this study is the presence of clay drapes along cell faces. More details about the method can be found in [17]. Figure 4 shows how the fine-scale pixel-based training image (left) is converted into an upscaled edge-based training image (right). The fine-scale training image has a grid cell size of 0.05 m and represents the clay drapes as consisting of pixels with a different pixel value than the background material. The upscaled edge-based training image has a grid cell size of 0.30 m and represents the clay drapes as edge properties that indicate the presence of clay drapes along the edges of all grid cells. The upscaled 30 m by 30 m training image from Figure 4 (right) is used as input to SNESIM from SGeMS to simulate clay drape realizations to be imported in the inner central zone of the model where individual clay drapes are incorporated. Vertical 2D realizations of 54.9m by 15.3m are generated. Figure 5 shows a random clay drape realization that is incorporated in the groundwater flow model. The realizations of clay drape presence can be imported in the groundwater flow code PMWIN using the Horizontal-Flow Barrier (HBF) package and the vertical leakance array (VCONT array). Initially, it is assumed that all clay drapes in the groundwater flow model have a thickness of 0.02 m and a hydraulic conductivity of 0.283 m/d. As mentioned previously, these values are optimized during calibration.

3. Results

Figures 6 and 7 show the resulting model outputs from the homogeneous model and the clay drape model. Both models were first manually calibrated. The optimal model from manual calibration was further calibrated using PEST [6] under different sets of constraints. For both models, automatic calibration using PEST did not result in lower calibration errors.

Figure 6 shows piezometric maps at z = 27 m TAW, i.e., located at the depth of the centre of the pumping well screen, for (1) the homogeneous and horizontally isotropic model and (2) the clay drape model. Figure 6 (left) shows circular hydraulic head contours indicating an isotropic piezometric pumping depression cone resulting from the homogeneity and isotropy of hydraulic conductivity in the horizontal direction. Figure 6 (right) shows the hydraulic head contours for the second model which incorporates clay drapes. These contours are elliptical demonstrating an anisotropic pumping depression cone. The vertical clay drapes cause bending of the hydraulic head contours. Since no other K heterogeneity than the clay drape presence is incorporated in the model, these results show that anisotropic pumping cones at large-scale can be attributed to the presence of small-scale clay drapes.

Figure 7 shows calculated versus observed drawdown graphs for (1) the homogeneous and horizontally isotropic model and (2) the clay drape model. The error variance for the isotropic model is 1.24 E-2, while the error variance for the clay drape model is as low as 7.292E-3. Incorporating the clay drapes results in a better fitting between calculated and observed drawdown values for this pumping test. Especially the larger drawdowns are better reproduced in the clay drape model. These large drawdowns are measured in observation well PB1.2 which is located close to the pumping well (Figure 2). In the clay drape model, a clay drape is present in the pumped layer between the pumping well and observation well PB1.2 which acts as a flow barrier between those two wells. The presence of this barrier results in a better reproduction of the measured drawdowns by the model.
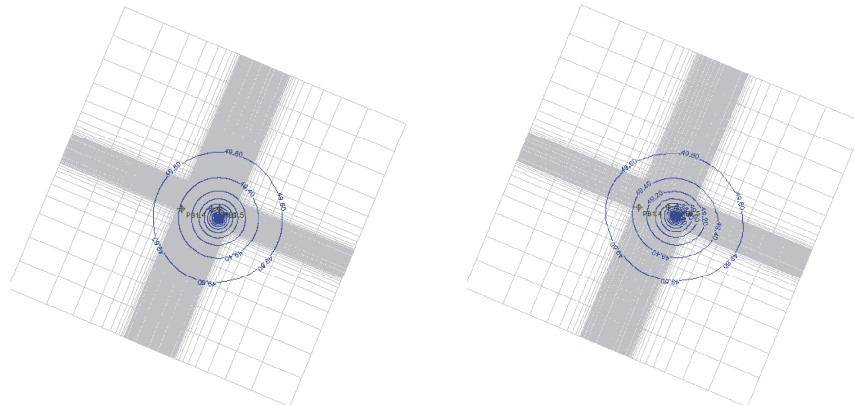
Figure 6 Piezometric maps at z = 27 m corresponding to the central level of the pumping well screen, for (1) the homogeneous and horizontally isotropic model and (2) the clay drape model showing drawdown after two days
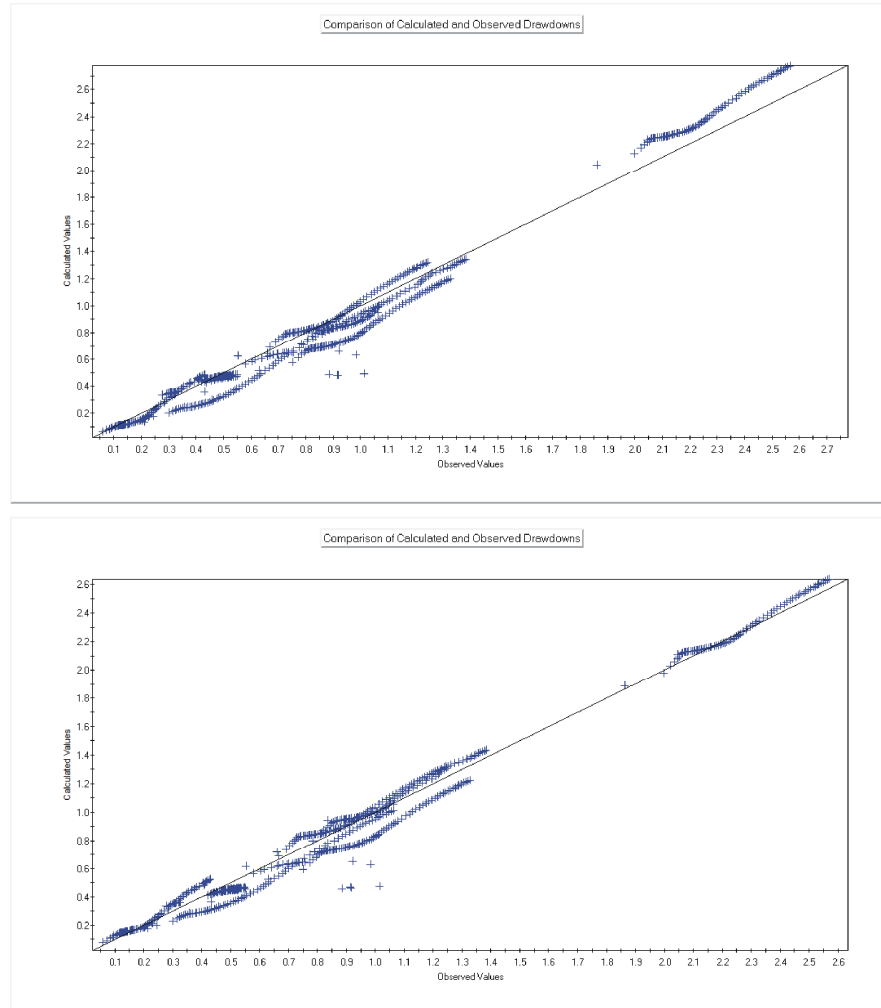
Figure 7 Calculated versus observed drawdown graphs for (1) the homogeneous and horizontally isotropic model and (2) the clay drape model

4. Discussion and conclusion

This study has investigated the effect of small-scale clay drapes on pumping test response. For this purpose, spatial distribution and geometry of clay drapes observed in a cross-bedded aquifer were explicitly incorporated in a local groundwater model of a pumping test site. Clay drape parameters were calibrated in order to reproduce hydraulic head measurements observed during a pumping

test. Best calibration results were obtained with a zoned clay drape parameter (hydraulic conductivity of drapes divided by drape thickness) with values between 0.175 and 9.905 day^{-1}. If the clay drape thickness is assumed to be 0.02 m, this means that hydraulic conductivity of the clay drapes is between 0.0035 m/day (= 4.05×10^{-8} m/s) and 0.1981 m/day (= 2.29×10^{-6} m/s). These values lie in the hydraulic conductivity interval of silt and silty sand respectively according to [9], so these values are realistic and are certainly not chosen unrealistically low. This means that with realistic values for clay drape thickness and hydraulic conductivity, the anisotropic pumping cone can be reproduced and explained. This shows that small-scale clay drapes can cause an anisotropic pumping test response at a much larger scale.

Incorporating clay drapes in groundwater models is challenging since they are often irregular curvilinear three-dimensional surfaces which may display a very complex spatial distribution. In this paper, a combined approach of multiple-point geostatistics and edge properties was used to incorporate the clay drapes in the flow model. Clay drapes were represented as grid cell edge properties instead of representing them by pixels. This allowed modelling with a larger grid cell size and thus a smaller CPU and RAM demand. A realistic spatial distribution of clay drape occurrence was simulated using multiple-point geostatistics based on a field-based training image. This combined approach of multiple-point geostatistics and edge properties has shown to be an efficient and valid approach since realistic spatial patterns and geometry of the clay drapes can be preserved in the model without having to represent each clay drape by pixels.

In order to determine the added value of explicitly incorporating clay drape presence in the flow model for pumping test interpretation, the model was also compared with a homogeneous and isotropic model calibrated on the same pumping test data. Incorporating the clay drapes resulted in a better fit between calculated and observed drawdown values than the homogeneous model.

Acknowledgements

References

[1]   Beliveau D., Reservoir heterogeneity, geostatistics, horizontal wells, and black jack poker, AAPG Bulletin 86 (10), 1847– 1848, 2002.

[2]   Caers J., and T. Zhang, Multiple-point geostatistics: a quantitative vehicle for integrating geologic analogs into multiple reservoir models, In: Integration of outcrop and modern analog data in reservoir models, AAPG memoir, vol 80, pp 383–394, 2004.

[3]   Chiang W. and W. Kinzelbach, 3D-groundwater modeling with PMWIN, Springer, Berlin. ISBN 3-540-67744-5, 2001.

[4]   Comunian A., Renard P., Straubhaar J. and P. Bayer, Three-dimensional high resolution fluvio-glacial aquifer analog – Part 2: Geostatistical modeling, Journal of Hydrology 405(1-2), 10-23, 2011.

[5]   dell'Arciprete D., Bersezio R., Felletti F., Giudici M., Comunian A., Renard P., Comparison of three geostatistical methods for hydrofacies simulation: a test on alluvial sediments, Hydrogeology Journal 20, 299-311, 2012.

[6]   Doherty J., Brebber L., and P. Whyte, PEST - Model-independent parameter estimation. User's manual. Watermark Computing. Australia, 1994.

[7]   Eaton T.T., On the importance of geological heterogeneity for flow simulation, Sedimentary Geology 184, 187–201, 2006.

[8]   Farmer C.L., Upscaling: a review, International Journal for Numerical Methods in Fluids 40(1-2), 63-78, 2002.

[9]   Fetter, C.W., Applied hydrogeology, Prentice-Hall, New Yersey, 598 p, 2001.

[10]   Harp D.R. and V.V. Vesselinov, Identification of Pumping Influences in Long-Term Water Level Fluctuations, Ground Water 49(3), 403-414, 2011.

[11]   Hendricks Franssen H.-J. and F. Stauffer, Inverse stochastic estimation of well capture zones with application to the Lauswiesen site (Tübingen, Germany), In Renard P., Demougeot-Renard H. and Froidevaux R. (Eds), Geostatistics for Environmental Applications, Proceedings of the Fifth European Conference on Geostatistics for Environmental Applications, Springer-Verlag, Berlin, Heidelberg, 2005

[12]   Houthuys R., Vergelijkende studie van de afzettingsstruktuur van getijdenzanden uit het Eoceen en van de huidige Vlaamse banken, Aardkundige Mededelingen 5, Leuven University Press, p. 137, 1990.

[13]   Houthuys R., A sedimentary model of the Brussels Sands, Eocene, Belgium, Geologica Belgica 14(1-2), 55-74, 2011.

[14]   Hu L.Y., and T. Chugunova, Multiple-point geostatistics for modeling subsurface heterogeneity: a comprehensive review, Water Resour Res 44:W11413, doi:10.1029/2008WR006993, 2008.

[15]   Huysmans M., and A. Dassargues, Hydrogeological modeling of radionuclide transport in low permeability media: a comparison between Boom Clay and Ypresian Clay, Environmental Geology, 50 (1), 122-131, 2006.

[16]   Huysmans M., and A. Dassargues, Application of multiple-point geostatistics on modeling groundwater flow and transport in a cross-bedded aquifer, Hydrogeology Journal 17(8), 1901-1911, 2009.

[17]   Huysmans M., and A. Dassargues, Direct multiple-point geostatistical simulation of edge properties for modelling thin irregularly-shaped surfaces, Mathematical Geosciences 43 (5), 521-536, 2011

[18]   Huysmans M., Peeters L., Moermans G., and A. Dassargues, Relating small-scale sedimentary structures and permeability in a cross-bedded aquifer, Journal of Hydrology 361, 41-51, 2008.

[19]   Kollet S.J. and V.A. Zlotnik, Influence of aquifer heterogeneity and return flow on pumping test data interpretation, Journal of Hydrology 300(1-4), 267-285, 2005.

[20]   Lavenue M. and G. de Marsily, Three-dimensional interference test interpretation in a fractured aquifer using the pilot point inverse method, Water Resources Research 37(11), 2659-2675, 2001.

[21]   Lebbe L. and W. Debreuck, Validation of an inverse numerical model for interpretation of pumping tests and a study of factors influencing accuracy of results, Journal of Hydrology 172(1-4), 61-85, 1995.

[22]   Mariethoz, G., Renard, P., Cornaton, F., Jacquet, O., Truncated plurigaussian simulations to characterize aquifer heterogeneity, Ground Water 47(1), 13-24, 2009.

[23]   McDonald M.G., and A.W. Harbaugh, A modular three-dimensional finite-difference ground-water flow model, Technical report USGS, Reston, VA, 1988.

[24]   Mikes D., Sampling procedure for small-scale heterogeneities (crossbedding) for reservoir modeling, Marine and Petroleum Geology 23 (9-10), 961-977, 2006.

[25]   Morton K., Thomas S., Corbett P., and D. Davies, Detailed analysis of probe permeameter and vertical inteference test permeability measurements in a heterogeneous reservoir, Petroleum Geosciences 8, 209-216, 2002.

[26]   Neuman S.P., Multifaceted nature of hydrogeologic scaling and its interpretation, Reviews of Geophysics 41 (3), 4.1– 4.31, 2003.

[27]   Peeters L., Fasbender D., Batelaan O. and A. Dassargues, Bayesian Data Fusion for water table interpolation: incorporating a hydrogeological conceptual model in kriging, Water Resources Research 46(8), DOI:10.1029/2009WR008353, 2010.

[28]   Renard Ph. and G. de Marsily, Calculating equivalent permeability: a review, Advances in Water Resources 20 (5-6): 253-278, 1997.

[29]   Ronayne M.J., Gorelick S.M., and J. Caers, Identifying discrete geologic structures that produce anomalous hydraulic response: An inverse modeling approach, Water Resources Research 44(8), DOI: 10.1029/2007WR006635, 2008.

[30]   Schulze-Makuch D. and D.S. Cherkauer, Variations in hydraulic conductivity with scale of measurement during aquifer tests in heterogeneous, porous carbonate rocks, Hydrogeology Journal 6 (2), 204– 215, 1998.

[31]   Schulze-Makuch D., Carlson D.A., Cherkauer D.S., and P. Malik, Scale depency of hydraulic conductivity in heterogeneous media, Ground Water 37(6), 904-919, 1999.

[32]   Strebelle S., Sequential simulation drawing structures from training images, Doctoral dissertation, Stanford University, 2000

[33]   Strebelle S., Conditional simulation of complex geological structures using multiple-point statistics, Math Geol 34:1–22, 2002.

[34]   Stright L., Modeling, Upscaling and History Matching Thin, Irregularly-Shaped Flow Barriers; A Comprehensive Approach for Predicting Reservoir Connectivity, SPE Paper 106528, 2006.

[35]   TUC RAIL N.V., Studie van de invloed van de tunnel voor de HSL op het grondwater van Bierbeek, internal report, 1993

[36]   Willis B.J. and C.D. White, Quantitative outcrop data for flow simulation, Journal of Sedimentary Research 70, 788-802, 2000.